Validation of the POLYPHEMUS platform: the ETEX, Chernobyl and Algeciras cases

Denis Quélo [a] Monika Krysta [a] Marc Bocquet [a] Olivier Isnard [b] Yannick Minier [b] Bruno Sportisse [a 1]

[a] *CEREA, Joint Laboratory Ecole des Ponts/EDF R&D*

[b] *Institute of Radiation Protection and Nuclear Safety, BP 17, 92262, Fontenay-aux-Roses, France*

Abstract

The objective of this article is to investigate the validity of a modeling system developed for forecasting atmospheric dispersion, the POLYPHEMUS platform, with a special focus on radionuclides. The platform is briefly described and model-to-data comparisons are reported for three cases: the ETEX campaign, the Chernobyl accident and the Algeciras release. The results are similar to those usually given in the literature by state-of-the-art models. Some preliminary sensitivity analysis indicate the main sources for uncertainties.

Introduction

A specific field of air quality modeling is related to risk assessment of accidental industrial releases. This concerns point emissions (local in space and time) of trace species that have zero or low atmospheric concentrations. In the late 80s and early 90s, considerable efforts have been devoted to the development of operational models, especially after the Chernobyl accident. There are now many available models

[1] Corresponding author

Preprint submitted to Elsevier Preprint

ranging from Gaussian-like models for short-range dispersion (and operational emergency centers, for instance [1,2]) to Lagrangian models and three-dimensional Eulerian models for long-range dispersion (see below).

Many models, based on state-of-the-art Chemistry-Transport Models (the so-called CTMs) have been developed, used or updated in this context (dispersion of radionuclides at regional scale). Model-to-data comparisons have been performed with a small set of observational data (typically the Chernobyl case and the ETEX campaign). Some model intercomparisons have also been performed (the ATMES exercise for instance, [3]). Among many other models, we can for instance cite the NAME ([4]), EURAD ([5]) or DREAM ([6]).

Modern numerical systems are supposed to have many features. A forecast has of course to be performed, before all. Many other high-level applications are also required, especially for risk assessment: getting an estimation of uncertainties through ensemble modeling or Monte Carlo simulations, inverse modeling of unknown emissions, data assimilation of observational data, etc. As such, the numerical model is only a "small" component of such systems.

The POLYPHEMUS platform has been developed in this context. The key motivation is a clear partitioning between different tasks: parameterizations and preprocessing of meteorological fields, model drivers (for forecast, for data assimilation, for ensemble simulations), models (especially the Chemistry-Transport model POLAIR3D, [7]) and post-processing tools (for instance for ensemble statistics). The POLYPHEMUS system has already been used for many applications with a focus on air quality: sensitivity analysis of ozone with respect to emissions ([8]), evaluation of uncertainties ([9]), inverse modeling of NOx emissions at regional scale ([10]), ensemble forecast for ozone ([11]), modeling of mercury and heavy metals at continental scale ([12,13]), etc.

The objective of this paper is to report preliminary validations of the POLYPHEMUS platform applied to the dispersion of radionuclides. Preliminary applications have been performed by former versions of the POLAIR3D model (for instance in [14,15] towards the ETEX data).

As in [16], the case studies are the ETEX campaign, the Chernobyl accident and the Algeciras release. Notice that this study is a first step before the operational use of the POLYPHEMUS system for the future emergency system for long-range dispersion of radionuclides at IRSN (Institute of Radiation Protection and Nuclear Safety).

This paper is organized as follows. Section 1 briefly describes the POLYPHEMUS platform with a focus on dispersion of radionuclides. Sections 2, 3 and 4 detail the applications to the ETEX campaign, the Chernobyl accident and the Algeciras release, respectively. Model-to-data comparisons are performed on the basis of available observational data. Some preliminary sensitivity analysis are also performed in order to underline the robustness and the limitations of the system. The article ends with a conclusion. Some future planned developments are also summarized with a focus on aerosol modeling, data assimilation and ensemble techniques.

1 Description of the POLYPHEMUS platform

1.1 Structure

The POLYPHEMUS platform is made of four components:

- physical parameterizations and preprocessing of input fields (meteorological fields, boundary conditions and emissions) are performed with the ATMODATA library. The purpose of the ATMODATA library is to perform the preprocessing of input fields, especially of meteorological fields (from Numerical Weather Forecasts or from mesoscale models). It does not depend on the numerical model.

  The outputs are typically the gridded data to be used for the dispersion: wind field V, vertical diffusion K_z, air density ρ and parameterizations for scavenging processes. These fields are given for the grid of the model (in the case of this article: the Chemistry-Transport Model POLAIR3D).

- drivers for high-level uses of models (driver for Monte Carlo simulations, driver for ensemble forecast (similar to [17,18]), driver for sequential data assimilation, driver for variational data assimilation [19,20,21]) have been defined in order to handle high-level uses of models. These drivers do not depend on the chosen model. Part of this level is still a work in progress.
- models (especially the Chemistry-Transport Model POLAIR3D, [7]) constitute the third level of the system. Other models can be plugged into the system. This is already the case for Gaussian-like (plume and puff) models used for risk modeling.
- the last level is composed of postprocessing tools, especially with the Python module ATMOPY. This library (which does not depend on the previous components) performs model-to-data comparisons and ensemble computations when required (the combination on the basis of appropriate algorithms of different model outputs).

1.2 The POLAIR3D *Chemistry-Transport Model*

The POLAIR3D CTM is basically a numerical solver of the reactive dispersion equation for the concentration of the trace species c_i (labeled with i):

$$\frac{\partial c_i}{\partial t} + \mathrm{div}\,(V\nabla c_i) = \mathrm{div}\left(\rho\, K \nabla\left(\frac{c_i}{\rho}\right)\right) - \Lambda_i^s\, c_i - \Lambda_i^d\, c_i + S_i \quad (1)$$

with Λ_i^s the wet scavenging coefficient, Λ_i^d the radioactive decay and S_i the point source for species i. K is the eddy diffusivity matrix, supposed to be diagonal. The vertical component is given by K_z (the default parameterization is the Louis parameterization, [22]). The horizontal component has a constant value K_H (in this study, $K_H = 0$).

Some boundary conditions have to be specified, especially at ground:

$$-K_z \nabla c_i \cdot \mathbf{n} = E_i - v_i^{dep} c_i \quad (2)$$

where $\mathbf{n}$ is the upward oriented unitary normal vector and E_i is the surface emissions for species i (0 in this case).

POLAIR3D solves the dispersion equation with an operator splitting method with many available options. In this specific case the source term is linear so there is no impact of the splitting strategy.

The advection step is solved with a third-order Direct Space Time scheme with a Koren-Sweby limiter function. The three directions are solved simultaneously. Because of the sharp gradients generated by the point-wise source, it is important that the advection scheme relies on a flux limiter. The diffusion step is solved with an implicit model (a second-order Rosenbrock method) with a three-points stencil for spatial discretization. Directional splitting is used. The scavenging step and the radioactive decay step are solved analytically. The ground boundary conditions are added to the diffusion step.

We refer to [7] for a deeper description of POLAIR3D. A general overview of algorithms is given in [23] and a comprehensive investigation of numerics in POLAIR3D may be found in [24].

1.3 Some specific parameterizations

1.3.1 Radionuclides

In these first applications, the only radionuclides taken into account are cesium and iodine. Two isotopes of cesium are modeled: ^{134}Cs and ^{137}Cs. Iodine is known to be in many possible forms (elemental gas-phase iodine, organic methyliodine or particle-bound iodine). We only consider one lumped form for ^{131}I. In order to be able to evaluate radiological consequences (doses), a comprehensive set of radionuclides will be added in the future.

1.3.2 Gas/aerosol modes

There are two modes of the model configuration for the dispersion of radionuclides :

- in a first mode, the trace species are supposed to act as gases;

- in a second mode, some trace species act as monodisperse aerosols. As such, they have a gravitational settling velocity and specific scavenging properties as functions of the particle size.

POLAIR3D may host two aerosol models: MAM, a Modal Aerosol Model and SIREAM, a Size Resolved Aerosol Model. These models solve the General Dynamics Equation for aerosols, by taking into account Brownian coagulation, condensation/evaporation and nucleation. Due to the lack of data for radionuclides, these models are not used for this application even if the attachment to atmospheric aerosols is known to be a key process for long-range dispersion ([25]).

1.3.3 Scavenging parameterizations

Resistance models for dry deposition and microphysical parameterizations for wet scavenging are available in the model. For a preliminary evaluation of the system, we have chosen to use a simple approach:

- a constant dry deposition velocity $v^{dep} = 0.2$ cm/s for cesium, $v^{dep} = 0.5$ cm/s for iodine;
- a scavenging coefficient parameterized as $\Lambda^s = A\,p_0^B$ with $A = 8.10^{-5}$, $B = 0.8$ and p_0 the rain intensity (in mm/hr).

We refer to [6,16,26] for comprehensive studies of these parameterizations.

1.3.4 Radioactive decay

The radioactive decay is only taken into account for the three trace species. The following values (in s^{-1}) have been used:

$$\Lambda^d_{^{131}I} = 9.97 \times 10^{-7}\ ,\quad \Lambda^d_{^{134}Cs} = 1.08 \times 10^{-8}\ ,\quad \Lambda^d_{^{137}Cs} = 7.32 \times 10^{-10} \tag{3}$$

which correspond to lifetimes of 8 days, 2 years and 30 years for ^{131}I, ^{134}Cs and ^{137}Cs, respectively.

In a future version, a comprehensive mechanism for radioactive fil-

iation will be added thanks to the Bateman's formula, which gives analytical solutions.

1.4 Operational set-up

The POLYPHEMUS platform will be fully operational at the Crisis Center of the French Institute of Radiological Protection and Nuclear Safety in the beginning of 2007. It will be a component of a modeling system KRX devoted to long-range (the LDX system) short-range (the PX system) atmospheric dispersion and radiological dose evaluations. In this configuration, POLYPHEMUS will be coupled to a meteorological server which will provide operational forecasting from Meteo France and ECMWF and detailed forecasting with the MM5 mesoscale model, to be runned on a cluster of 40 processors.

1.5 Statistical indicators

Accidental releases of pollutants are described statistically quite differently from diffuse pollutants (passive or reactive). This is mainly due to the obvious statement that the pollutant forms a clear-cut cloud in the short term. As a consequence the concentration profile at a given station is made up of smoothed peaks giving away the cloud passings. Therefore statistical indicators measuring the skills of a model simulating releases should be adequate. Specifically classical indicator such as correlation coefficients, bias, figure of merit, normalized mean square error, should not apply only to concentrations, maximum concentrations, or dosage (time-integrated concentrations), but also to the following relevant observables :

- The *arrival time* of the cloud which is the first time the concentration in tracer exceeds the background value threshold.
- The *arrival time of maximum concentration* which measures time when the maximum concentration at the station occurs.
- The *duration coefficient* which is the time spent by the concentration

at a given station above a threshold.

Qualitative global scatter diagrams can be used on those observables, as well as the classical statistical indicators mentioned above. A comprehensive description of the indicators which were applied to the simulations can be found in Appendix.

2 Application to the ETEX campaign

2.1 The ETEX campaign

The European Tracer EXperiment (ETEX) is one of the best instrumented dispersion experiment at continental scale to date. Moreover, it is well documented ([27], and online documentation : `http://rem.jrc.cec.eu.int/etex/`). It has followed the ATMES (Atmospheric Transport Model Evaluation Study) program, which was intended to test models capabilities to simulate the dispersion of the radionuclides (^{131}I and ^{137}Cs) released and transported during the Chernobyl accident. The ETEX experiment was conducted in 1994 by the European Joint Research Centre. It decomposed into two distinct exercises ETEX-I and ETEX-II. As in many works, applications to the first campaign will be emphasized since the results of the second experiment are known to be much more difficult to interpret.

As for ETEX-I, 340 kilograms of Perfluoromethylcyclohexane (PMCH) were released uniformly from 23/10/1994 1600UTC to 24/10/1994 0350UTC, at Monterfil (Brittany, France, located 48°03′ N, 2°00′ W). This compound was chosen because it is safe, inert, and is hardly removed by wet scavenging or dry deposition. Besides, it can be measured down to very low concentration levels. It has a residual background value in the atmosphere of about $0.05\,\mathrm{ng.m^{-3}}$. At the time of the release, the meteorological conditions were driven by a depression over Scotland. The main wind direction was north-east bound.

Many European research teams were involved in taking measurements

to characterize the dispersion of the PMCH cloud over Europe. 168 WMO stations over 17 countries, owned by the local meteorological services, participated in the observation campaign, yielding 969 measurements of PMCH concentrations above PMCH background level and 2136 others (quality control checked) concentrations within the background PMCH noise level. The results of the experiment were used to calibrate various atmospheric dispersion models. In particular, the ATMES II inter-comparison exercise (43 participants) focussed on ETEX-I. Many modeling and comparison to data results were also collected in the special issue of *Atmospheric Environment,* **32,** issue 24, 4089–4375, 1998. It was the central topic of the long-range transport, model verification and emergency response which took place in Vienna in 1997 ([28]).

Alternatively these measurements were used to test source inversion methods on a real and well instrumented dispersion event. Among the contributions on the subject [29,30,31,14,32,15], several were using POLAIR3D, the CTM of the POLYPHEMUS system.

2.2 Set-up

For the simulation presented here, the domain was chosen large enough so that outgoing PMCH is not significantly tampering the simulation for at least several days. The center of the south-west corner cell is at $-20°$W, $36,05°$N. It was chosen so that the ETEX release point be at the center of a cell.

The finest meteorological fields were provided by the ECMWF at the resolution $0.5° \times 0.5°$. These are operational fields. For the purpose of the simulation ahead, we use ERA-40 fields, with a lower resolution of $1.125° \times 1.125°$, but a greater confidence (these are re-analyzed fields). The time-step is 3 hours.

The resolution of the simulation may differ from the meteorological fields resolution (the meteorological fields are then interpolated). A finer nested Lagrangian model operating in the vicinity of the source

observable vs. indicator	correlation	FM	NMSE	FB
dosage	0.80	0.32	6.27	0.93
arrival time	0.94	0.90	0.13	-0.023
duration	0.74	0.66	0.54	0.11
maximum	0.83	0.37	3.84	0.75
peak time	0.58	0.77	0.92	0.15

Table 1
Statistical indicators for the dosage, arrival time, duration, maximum concentration and arrival time of maximum concentrations.

may make a difference. For the simulation ahead, the resolution is chosen to be $0.5° \times 0.5°$ with a time step $\Delta t = 600$ seconds. The number of cells is $N_x = 137$ and $N_y = 73$.

For this simulation, 12 vertical levels are taken into account, up to 6090 m.

2.3 Results and discussion

We have evaluated our simulation against the observations at stations with a minimum of 11 measurements. There are 139 such stations. On Fig. 1, we have plotted the scatter plots for dosage, arrival time, duration (total time above 0.05 ng.m^{-3}), maximum concentration and arrival time of maximum concentrations. Unlike the ATMES II exercise, the emphasis is not so much on the concentrations statistics but rather on the statistics of the observables built on those concentrations, as was advocated in [33]. The statistical indicators which have been computed for these observables are given in Tab. 1

When considering all concentration measurements of the same 139 stations, the correlation is 0.60, the FM is 0.26, the NMSE is 5.00, the FB is 0.89. When considering all measurements, the correlation is 0.58, the FM is 0.28, the NMSE is 3.98, the FB is 0.81. These statistics compare well with state-of-the-art models ([33]).

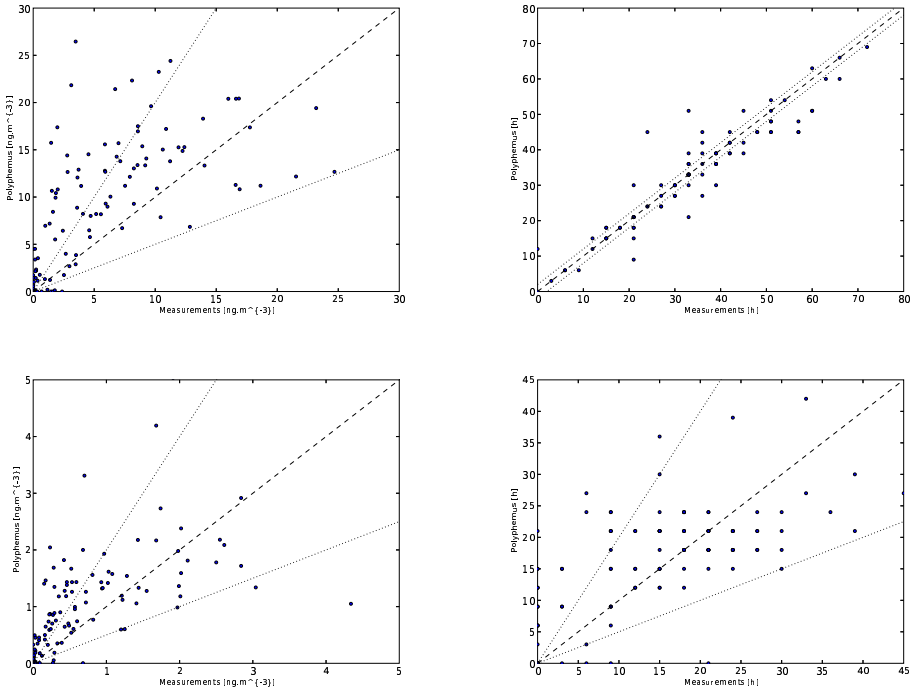

Figure 1. Scatter plots of the dosage (top left), arrival time (top right), maximum concentration (bottom left) and duration (bottom right) computed on the set of 139 stations of the ETEX-I release.

However the model is incline to overestimate the station dosages of PMCH (the fractional bias being 0.93).

3 Application to the Chernobyl accident

An explosive accident took place at the Chernobyl nuclear power plant unit IV in Ukraine (51°17′ N, 30°15′ E) on 25 April 1986 at 2123 UTC. This accident led to a widespread dispersion of radionuclides in the atmosphere at the continental scale. Most of the released material was in particulate form except for noble gases and the majority of iodine. Radioactivity was measured in many European countries after the accident.

3.1 Set-up

3.1.1 Emission data

Contrary to the ETEX campaign, the estimate of the emissions are still highly uncertain: this concerns the total released activity, the time distribution (most of the release occurred during the period 25 April-5 May) and the vertical distribution. Notice that the estimation of the source term has been several times corrected by more than a factor of two and that [6] reports an uncertainty of at least 50 %.

The key uncertainty is related to the vertical distribution of the emissions: due to the high temperature of the core, the material was assumed to reach heights up to 2000 meters, probably more. The effective release height changed considerably during the release: the initial explosion lifted material to high altitude while release heights were probably much lower in the next two weeks.

In our runs we have chosen to follow the recommendations of [34] for the time distribution and the total released activity, and of [6] for the vertical distribution. The time evolution and the vertical distribution we have used are given in Table 2.

	26/4	27/4	28/4	29/4	30/4	1/5	2/5	3/5	4/5	5/5
t	0.40	0.116	0.085	0.058	0.039	0.035	0.058	0.061	0.074	0.074
z_1	0.	0.	0.	0.	0.	0.	0.	0.	0.	0.
z_2	0.	0.	0.2	0.2	0.2	0.2	0.2	0.2	0.2	0.2
z_3	0.	0.1	0.5	0.5	0.5	0.5	0.5	0.5	0.5	0.5
z_4	0.	0.5	0.3.	0.3	0.3	0.3	0.3	0.3	0.3	0.3
z_5	0.4	0.4	0.	0.	0.	0.	0.	0.	0.	0.
z_6	0.3	0.	0.	0.	0.	0.	0.	0.	0.	0.
z_7	0.2	0.	0.	0.	0.	0.	0.	0.	0.	0.
z_8	0.1	0.	0.	0.	0.	0.	0.	0.	0.	0.

Table 2
Time and vertical distribution for Chernobyl emission. The levels z_i are: 32, 150, 360, 640, 990, 1400, 1800 and 2300 meters.

Even if the radionuclide composition is known to have been very complex, we have chosen to describe only iodine (^{131}I) and cesium (with the two isotopes ^{134}Cs and ^{137}Cs).

Another key uncertainty is the partitioning among particulate phase and gaseous form. We refer to [25] for a comprehensive study of the radioactive particles from the Chernobyl accident. The impact of large particles (aerodynamic diameters larger than 20 μm) is investigated. Another interesting feature pointed out by this article is the trade-off between effective release height higher than usually reported and vertical upwards motions due to convective cells with rising currents of warm air (especially during April 26 over Belarus and Baltic states). Notice that we have not included the description of convective motions in our dispersion model.

3.1.2 Meteorological data

Weather conditions during the release are well documented. A high-pressure center with strong inversion at about 500 meters was active over the site.

The meteorological data used as inputs for the POLYPHEMUS system are ERA-40 data from ECMWF with a $1.125° \times 1.125°$ horizontal resolution. The time resolution is 3 hours and there are 61 vertical levels (hybrid coordinates).

In some configurations of the runs, we have also used meteorological data computed by the MM5 mesoscale model (version v5.2). The concern was mainly to investigate the sensitivity with respect to rain intensity and many microphysical schemes parameterizing cloud and rain processes in MM5 have been tested. For the sake of clarity, the results are not reported here and we refer to a future paper.

3.1.3 Numerical set-up

The horizontal grid is made of 66×31 cells ($1.125° \times 1.125°$ horizontal resolution). The vertical grid of POLAIR3D is made of 12 levels with the following heights of the interfaces: 62, 236, 484, 796, 1184, 1616, 1984, 2616, 3184, 3616, 4384 and 5016 meters. The timestep is 600 seconds.

3.1.4 Measurements

The measured data are provided by the REM-database at the Environment Institute (Joint Research Center, Ispra, Italy). They consist of data from 88 stations. This represents up to 1278 observational data for cesium and 1333 observational data for iodine (whatever the measurement duration is). The map of stations is given in Figure 2 (bottom right). The diameter of the circle indicates the magnitude of the maximal measured value for the station.

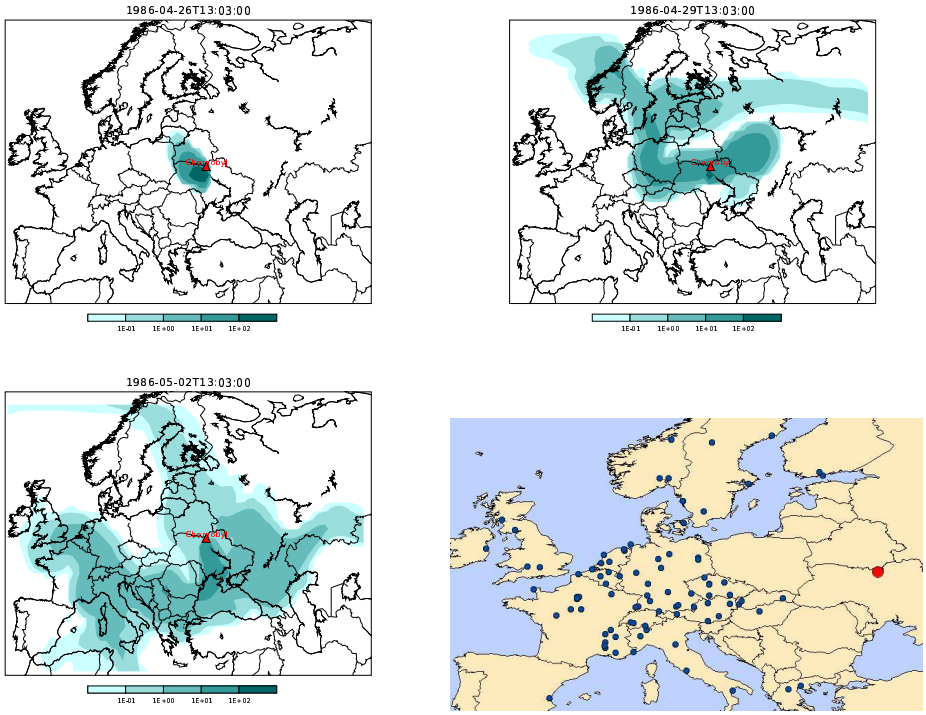

Figure 2. Chernobyl accident: maps of ground concentrations of ^{137}Cs (in Bq/m^3) at 1300 UTC on 26 April (top left), 29 April (top right) and 2 May (bottom left). The map of stations is given bottom right.

3.2 Results and discussion

Maps of the computed surface concentration of ^{137}Cs are given in Figure 2 for 26 April, 29 April and 2 May (13:00 UTC), respectively (one, four and seven days after the start of the release). The plume location is coherent with the meteorological understanding and with similar maps reported in the literature.

Model-to-data comparisons are illustrated by Figure 3 with a scatter plot of ^{137}Cs. The arrival time is well computed as illustrated (notice that the arrival time is computed for the observational data as the first time for which the observed value is above a given threshold: the computed arrival time is only defined for times with *available* data).

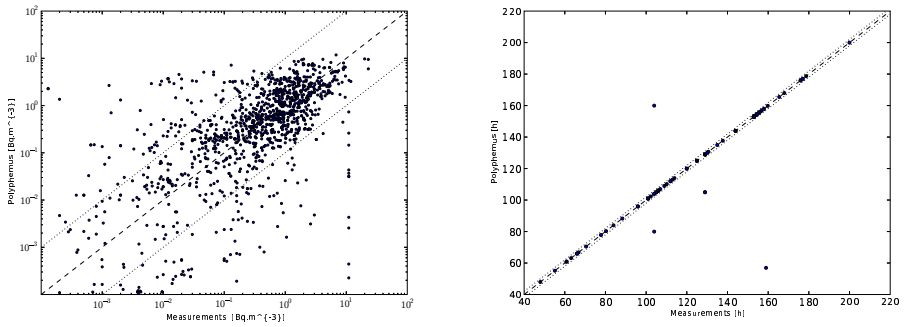

Figure 3. Chernobyl accident. Results for the simulation of ^{137}Cs. Scatter plot for activity concentrations in logarithmic scale (left) and for the arrival time (right).

This means that when a station indicates for the first time radioactivity, the model output also indicates radioactivity. Notice that the quality of this indicator is not as meaningful as for the ETEX case (for which the data are available during the whole period).

Specific results for each station are available on request (but not reported here due to the length of the table -more than two pages). Some typical model-to data comparisons are illustrated in Figure 4. Error statistics are reported in Table 3.

species	obs. data	obs. mean	sim. mean	correlation	NMSE
^{131}I	1333	3.872	8.142	44.86%	1.397
^{137}Cs	1278	1.103	1.111	45.5%	1.146

Table 3
Error statistics for Chernobyl accident

To date, the most comprehensive modeling studies (up to our knowledge) devoted to the Chernobyl accident are those of [6]. These results are similar to those obtained in these studies.

Notice that these results are particularly sensitive to the source term. For instance, with the time distribution used in [6], the correlation for iodine and cesium is 35 % and 38.5 %.

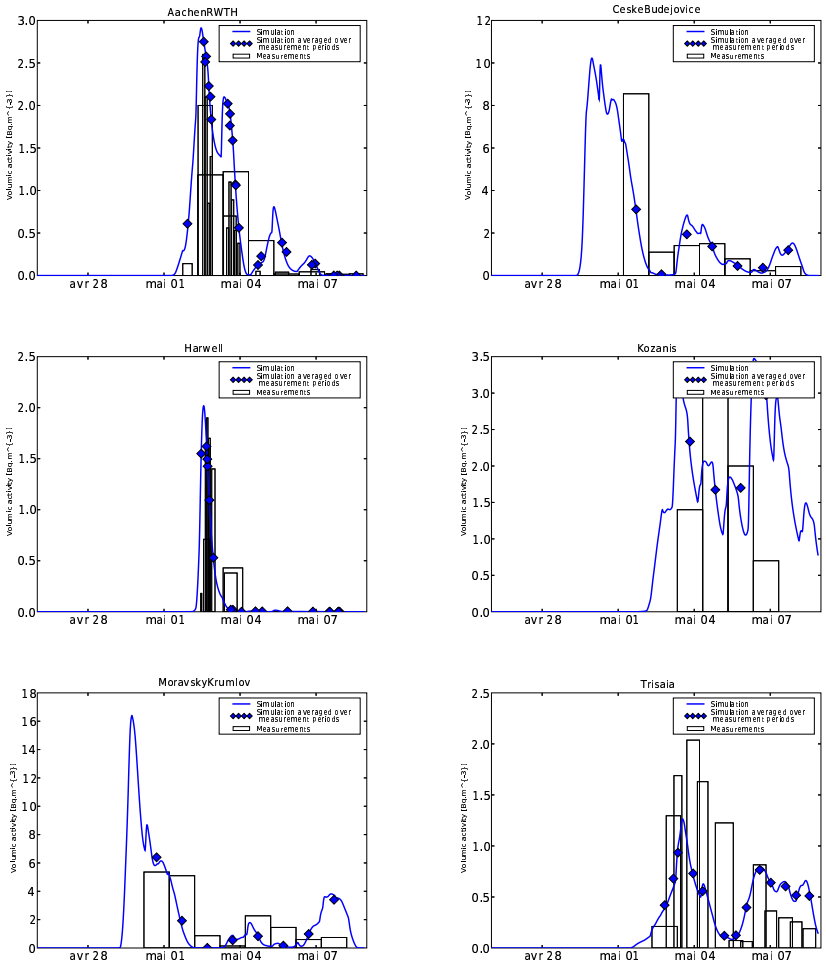

Figure 4. Chernobyl accident: concentration of ^{137}Cs activity expressed in Bq.m^{-3} as measured (rectangles) and predicted by the model. The solid line illustrates instantaneous profile and diamonds stand for model values corresponding to the measurements. From left to right and from top to bottom the stations are : Aachen RWTH, Ceske Budejovice, Harwell, Kozanis, Moravsky Krumlov, Trisaia.

4 Application to the Algeciras release

In late May and early June 1998 monitoring networks of several European countries detected elevated levels of radioactivity in the atmo-

sphere. The highest values have been recorded in the south of France and north of Italy. Several days afterwards it was established that they resulted from a release that had taken place in a steel mill located in the south of Spain. The Acerinox furnace planted in between Algeciras and Gibraltar melted accidentally a radiotherapy source of ^{137}Cs. The release was qualified as incident by the IAEA.

4.1 Set-up

4.1.1 Simulation

To our knowledge, the first attempt to simulate consequences of the incident came from the Lawrence Livermore National Laboratory. On the basis of model-to-data comparison [35] attempted to establish the time of the release and the rejected activity. [36] and, to a larger extent, [26] focused on the influence of refinement of dry and wet deposition schemes. The latter report presents simulations that took place within the RTMOD exercise, [37].

The results of the simulation presented in this paper have been obtained with the POLYPHEMUS platform. The domain of computation is spanned by the intervals $[18°15'\mathrm{W}, 27°15'\mathrm{E}] \times [26°45'\mathrm{N}, 59°45'\mathrm{N}]$. The mesh consists of 91×66 cells at each of 14 vertical layers. It covers the location of the accident ($5°26'\mathrm{W}, 36°10'\mathrm{N}$) and extends over the whole area where the measurements were collected. ECMWF operational meteorological fields with spatial resolution of $0.5° \times 0.5°$ and 6h frequency have been used in this simulation. Following the studies in [26] the time of the release has been chosen between 0130 and 0200 UTC on 30 May 1998 and the quantity of the released activity equals to 1.85×10^{12} Bq. Due to the elevation of the release point resulting from the presence of a stack the source has been placed at the second level, ie between 64 and 236 meters.

Dry deposition is parameterized with constant velocity equal to $v_d = 0.1\,\mathrm{cm.s^{-1}}$. This value gives better results than the default value 0.2 $\mathrm{cm.s^{-1}}$, which justifies its use in this case. Due to lack of information

concerning rainfall in the operational ECMWF fields, scavenging has been ignored. Radioactive decay of ^{137}Cs has been taken into account.

4.1.2 Measurements

It is agreed today that it took place between 0100 and 0300 UTC on 30 May 1998. The estimated quantity of the released radioactivity is known up to an order of magnitude $[2.96 \times 10^{11}, 2.96 \times 10^{12}]$ Bq.

118 mean activity concentrations in air have been measured. For each measurement the date of the beginning and the end of the measurement interval has been reported. No more precise information has been given however. Common sense makes one suppose it started at 1200 UTC on the first day and the ended at 1200 UTC on the last day. The same hypothesis has been made in [35]. The measurement intervals cover periods of between 1 and 14 days and in some places they start even before the release took actually place.

The localization of the monitoring stations is shown in Fig 5. Half of the measurements come from the stations where one measurement only has been taken. For the remaining half two or more values have been recorded. The monitoring stations in several places in France and Italy, Fig. 8 and Fig. 7 respectively, have recorded up to 5 daily measurements. Their values reflect the shape of the passing cloud.

4.2 Results and discussion

First, the development of the simulated plume can be followed in Fig. 6. Several maps of Europe presented in this figure show the plume's extent every 12 hours. The first one illustrates the cloud at 1200 UTC on 30 May 1998, 10 hours after the end of the release. The last one dates from 0000 on 5 June 1998.

Simulation results show eastward plume advection over the Mediterranean Sea in the first phase after the accident. It explains the scarcity

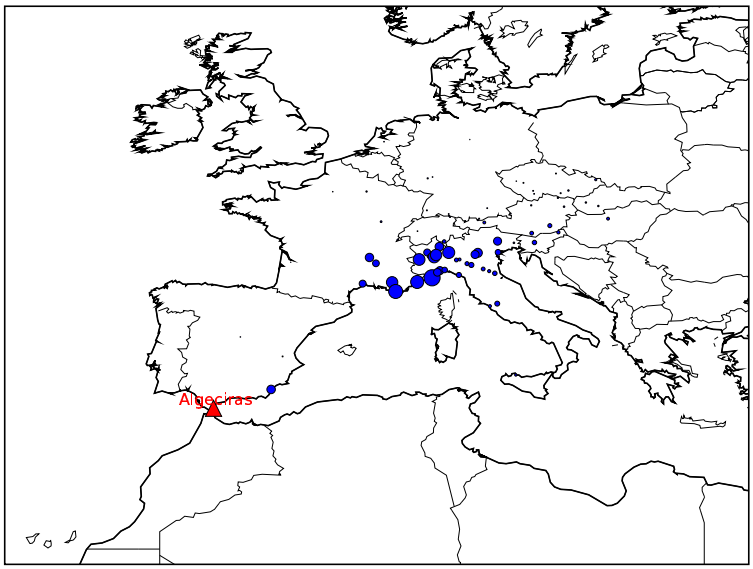

Figure 5. Monitoring stations for the Algeciras incident are drawn with circles. Circle diameter corresponds to the value of the largest measurement taken at a given point. Source localization in Algeciras is marked with a triangle

of measurements over the Spanish territory. Large discrepancy between the measured and observed value in Gibraltar reflects significant model error in the vicinity of the source. Further downwind however, along the Spanish coast, we note better model-to-data correspondence. Moreover, our model predicts correctly the arrival time at southern France and northern Italy on 2 June 1998, Fig. 8 and Fig. 7. Model results for Nice match quite well the measurements. Those for Cadarache and Montpellier constantly overpredict them. Next, the plume moves towards Switzerland and Italy. The temporal profile of the passing cloud, both its shape and concentration values, are reproduced reasonably well for the Italian station of Ispra, Fig. 7. The shape of the modeled profile resembles to the measured one for Capo Mele and Vercelli. It is however totally off for Trino. Two possible reasons behind it could be conjured. Firstly, it might be due to a stagnant

cloud that has been trapped somewhere between the mountains. The second possible explanation is a mistake in the reported measurement dates. Trino lies only 20 km from Vercelli and roughly half-way between Torino and Milan. Curiously enough, the concentrations that have been recorded there are shifted towards later times with respect to the surrounding stations.

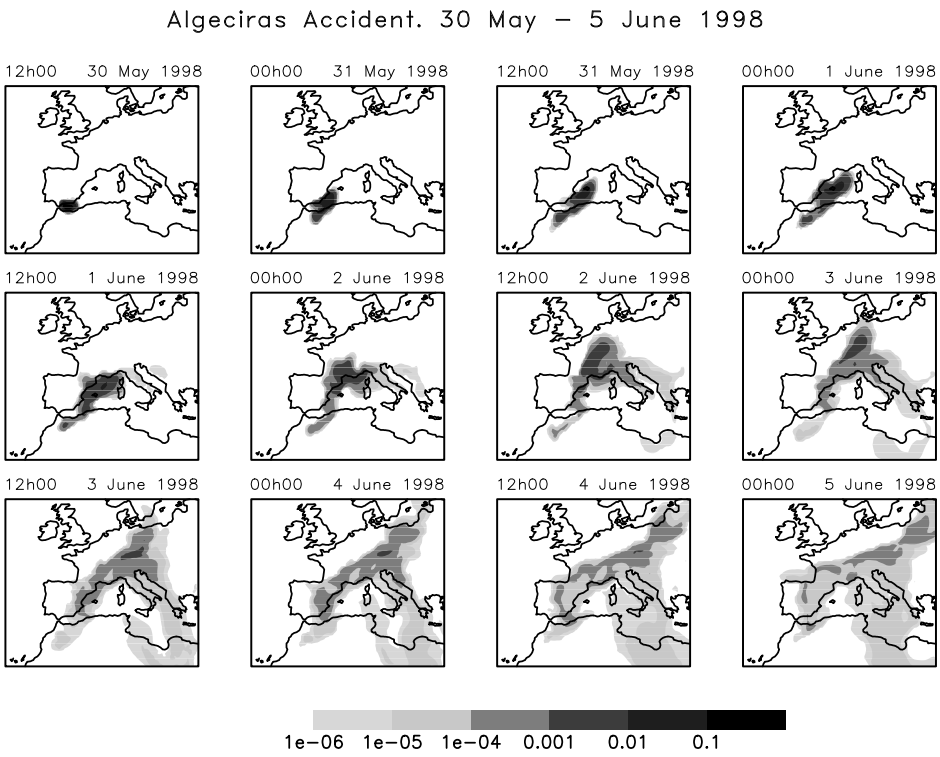

Figure 6. Plume of ^{137}Cs for the Algeciras accident. Activity concentrations are expressed in Bq.m^{-3}

Monitoring stations scattered over Central Europe were swept by a well-spread and diluted cloud and consequently less severely contaminated than those in France or Italy. Not only were they at large distances from the source but also collected usually no more than one measurement averaged over a period of several days. Therefore, quality of the results for those sites is more difficult to evaluate.

Model-data comparisons for several monitoring stations are shown beneath. The selected stations have already been discussed and are those that captured the evolution of daily-averaged radioactivity concentrations.

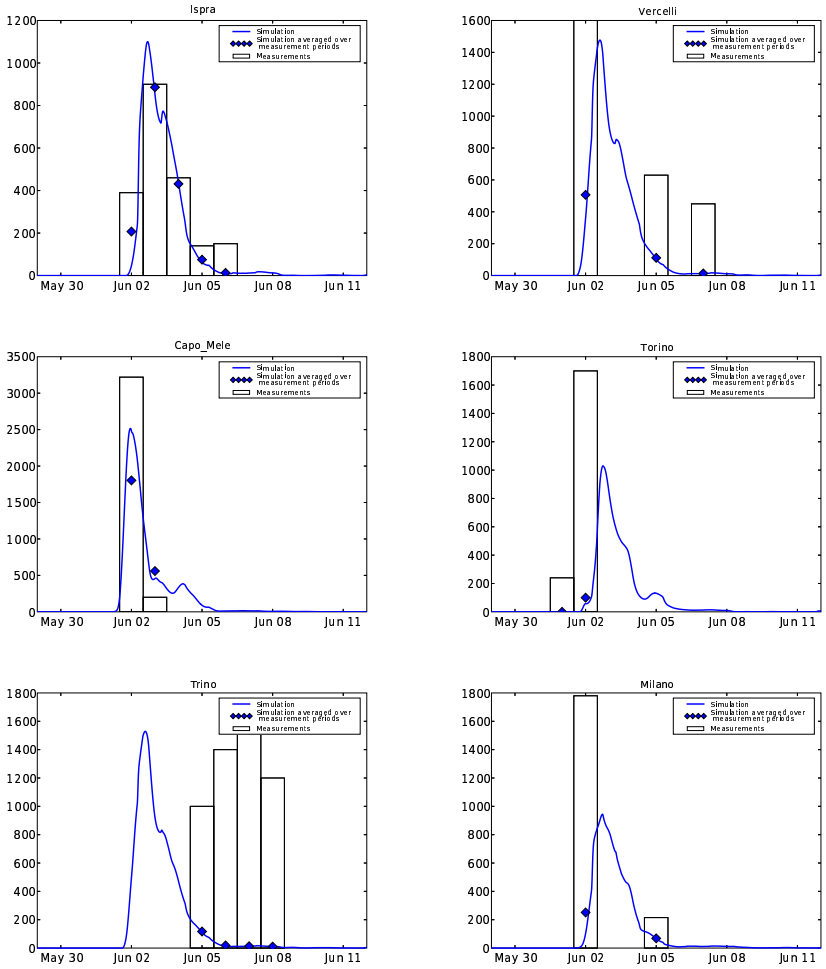

Figure 7. Concentration of activity expressed in μBq.m^{-3} as measured (rectangles) and predicted by the model. The solid line illustrates instantaneous profile and diamonds stand for model values corresponding to the measurements. From left to right and from top to bottom the stations are : Ispra, Vercelli, Capo Mele, Torino, Trino and Milano

In Fig.9 a global correspondence between the simulated air concentra-

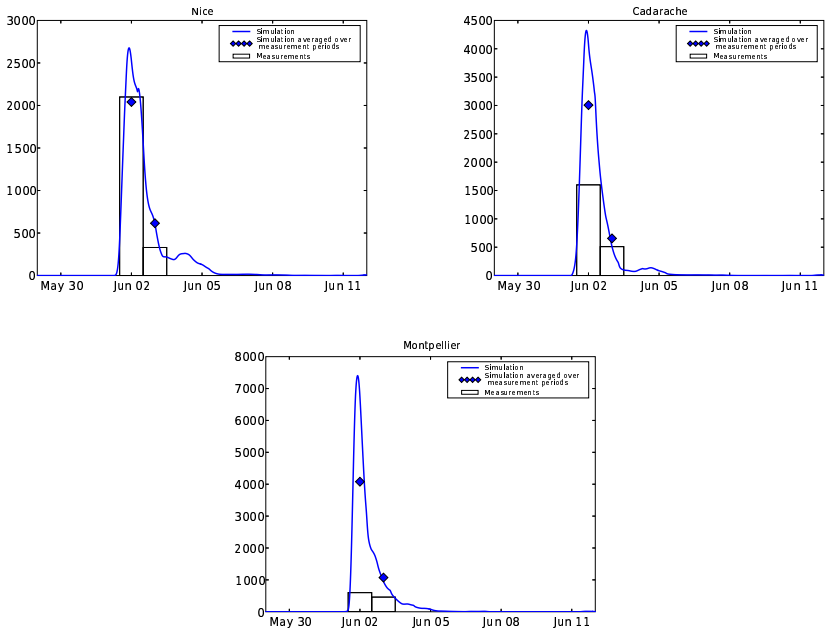

Figure 8. Profiles of activity concentration, μBq.m^{-3} in Nice, Cadarache and Montpellier in the south of France. The measurements are represented with the rectangles, the solid line represents the simulated profile and diamonds stand for measures as predicted by the model

tions and the measured ones is illustrated for all 118 available measurements. The majority of the points are situated between two dotted lines. It implies that for most of the monitoring stations model predictions come within an order of magnitude to the measurement. There are some however for which the discrepancies are higher. At the first sight one notices that the points are roughly uniformly distributed on both sides of the diagonal. Quantitatively this fact is reflected in the small values of bias, fractional bias and mean geometric bias, Tab. 4. The last quantity is particularly well adapted to the analysis of two data sets with large discrepancies like the ones for the Algeciras simulation. The distribution of the points around the diagonal of the scatter-plot might be uniform but the discrepancies are large. Therefore the statistical indicators based on variance, like the normalized mean square error, fractional standard deviation and geometric mean variance have higher values. The correlation of 20% is quite poor

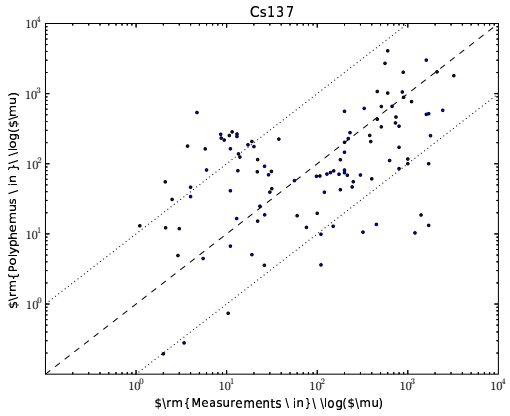

Figure 9. Scatter plot for model-to-data comparison in logarithmic scale

mostly due to the fact that no measurement selection has been done and all have been taken into account in the validation procedure. It is enough to get rid of the two measurements in the close vicinity of the source so that is rises up to 46%.

The set-up of the simulation illustrated in Fig. 6 consists in using operational meteorological fields of the ECMWF. Previously in this paper ERA-40 fields have been used and their merits discussed. Nevertheless, for the dispersion of radioactivity after the Algeciras release the simulation based on operational fields give better results than the one for ERA-40. It is clearly visible if one analysis the values of the statistical indicators as shown in Tab. 4. All of the values associated with the ERA-40 fields indicate much worse model performance.

Conclusion

A preliminary validation of the POLYPHEMUS system has been performed toward measured data the for the Chernobyl accident, the ETEX campaign and the Algeciras release. The statistical indicators for model-to-data comparisons indicate the good behavior of the system as compared to other state-of-the-art models.

Indicator	**ERA-40**	**Operational**
$\overline{M}[\mu\text{Bq.m}^{-3}]$	365.3	365.3
$\overline{P}[\mu\text{Bq.m}^{-3}]$	249.1	398.2
B $[\mu\text{Bq.m}^{-3}]$	-116.2	32.85
FB	-0.38	0.09
MG	4.34	1.55
NMSE	3.40	2.24
FSD	1.60	1.30
VG	203.6	53.1
ρ	-0.02	0.19
FM	0.11	0.29

Table 4
Model-to-data comparison for the Algeciras release. Statistical indicators asses the quality of a simulation based on the ECMWF ERA-40 and operational meteorological fields. Due to large discrepancies between model predictions and data geometric mean bias (MG) and geometric mean variance (VG) have been additionally reported. The indicators have been computed for 118 measurements. The only exception is VG which has been computed for 108 measurements. The measurements are those for which model prediction is higher than $1\,\mu\text{Bq.m}^{-3}$

POLYPHEMUS will be the basis of the coming operational system (ldX) used for long-range dispersion at IRSN (Institute of Radiation Protection and Nuclear Safety). Complementary works are also in progress. Sensitivity analysis are currently performed (following [6] for scavenging parameterizations and [8] for a comprehensive set of model configurations). A parameterized version describing aerosols to which radionuclides are bound is also developed. The issue is to have an improved description of the scavenging processes. Some works are also devoted to the opportunity of using data assimilation to improve forecast of radionuclides.

Acknowledgements

We thank our colleague Jean-Pierre Issartel for having initiated the ETEX runs at CEREA. We thank Stefano Galmarini (JRC, Ispra) for having provided the observational data of Algeciras release.

A Statistical indicators

The statistical indicators considered to be the most effective for the evaluation of the model-to-data comparison are defined in this section following [38] and [33].

We considered a set of measurements $\{M_i\}_{i=1}^N$ (mean $\overline{M}$) and the corresponding model outputs $\{P_i\}_{i=1}^N$ (mean $\overline{P}$).

- The bias (B) is defined as the average difference between the two sets of value

$$\mathrm{B} = \frac{1}{N}\sum_{i=1}^{N}(P_i - M_i) = \overline{P} - \overline{M} \tag{A.1}$$

  Its sign indicates an under or over prediction of the model with respect to the measurements.
- The fractional bias (FB) represents a relative difference between model outputs and measurements (comprise in $[-2, 2]$).

$$\mathrm{FB} = 2\,\frac{\overline{P} - \overline{M}}{\overline{P} + \overline{M}} \tag{A.2}$$

- The geometric mean bias (FB) is meaningful when the ratio between measurements and model outputs is large

$$\mathrm{MG} = \exp\left(\frac{1}{N}\sum_{i=1}^{N}\ln P_i - \frac{1}{N}\sum_{i=1}^{N}\ln M_i\right) = \prod_{i=1}^{N}\left(\frac{P_i}{M_i}\right)^{\frac{1}{N}} \tag{A.3}$$

- The normalized mean square error (NMSE) gives information on

the deviations. It is defined as

$$\mathrm{NMSE} = \frac{1}{N}\sum_{i=1}^{N}\frac{(P_i - M_i)^2}{\overline{P}\,\overline{M}} \tag{A.4}$$

- The geometric mean variance (VG) gives information on the deviations as well. It is defined as

$$\mathrm{VG} = \exp\left[\frac{1}{N}\sum_{i=1}^{N}(\ln P_i - \ln M_i)^2\right] \tag{A.5}$$

- The fractional standard deviation (FSD) is defined as

$$\mathrm{FSD} = 2\,\frac{\sigma_M^2 - \sigma_P^2}{\sigma_M^2 + \sigma_P^2} \tag{A.6}$$

where

$${\sigma_P}^2 = \frac{1}{N}\sum_{i=1}^{N}\left(P_i - \overline{P}\right)^2 \qquad \text{and} \qquad {\sigma_M}^2 = \frac{1}{N}\sum_{i=1}^{N}\left(M_i - \overline{M}\right)^2 \tag{A.7}$$

- The correlation coefficient ranges between -1 and $+1$. It is defined as

$$\mathrm{correlation} = \frac{\sum_{i=1}^{N}(M_i - \overline{M})(P_i - \overline{P})}{\sqrt{\sum_{i=1}^{N}(M_i - \overline{M})^2\,\sum_{i=1}^{N}(P_i - \overline{P})^2}}\,. \tag{A.8}$$

- The figure of merit (FM) is defined as

$$\mathrm{FM} = \frac{\sum_{i=1}^{N}\min(P_i, M_i)}{\sum_{i=1}^{N}\max(P_i, M_i)} \tag{A.9}$$

References

[1] Jürgen Päsler-Sauer. Description of the atmospheric dispersion model ATSTEP. Version RODOS PV 5.0. Technical Report RODOS(RA2)-TN(03)-01, Forschungszentrum Karlsruhe GMBH, 2003.

[2] S. Thykier-Nielsen, S. Deme, and T. Mikkelsen. Description of the atmospheric dispersion module RIMPUFF. Technical Report

RODOS(WG2)-TN(98)-02, Forschungszentrum Karlsruhe GMBH, 1999.

[3] W. Klug, G. Graziani, G. Gripa, D. Pierce, and C. Tassone. Evaluation of long range atmospheric transport models using environmental radioactivity data from the Chernobyl accident: the ATMES report. Technical report, Elsevier Applied Science, 1992.

[4] R.H. Maryon, F.B. Smith, B.J. Conwy, and D.M. Goddard. The UK nuclear accident response model (NAME). *Progress in nuclear energy*, 26(2):85:104, 1992.

[5] H. Haas, M. Memmesheimer, H. Geiss, H.J. Jacobs, M. Laube, and A. Ebel. Simulation of the Chernobyl radioactive cloud over Europe using the EURAD model. *Atmos. Env.*, 24A(3):673–692, 1990.

[6] J. Brandt, J.H. Christensen, and L. Frohn. Modelling transport and deposition or caesium and iodine from the Chernobyl accident using the DREAM model. *Atmos.Chem.Phys.*, 2:397:417, 2002.

[7] J. Boutahar, S. Lacour, V. Mallet, D. Quélo, Y. Roustan, and B. Sportisse. Development and validation of a fully modular platform for numerical modelling of air pollution: Polair3D. *Int. J. Env. and Pollution*, 22(1-2), 2004.

[8] Vivien Mallet and Bruno Sportisse. A comprehensive study of ozone sensitivity with respect to emissions over Europe with a chemistry-transport model. *J. Geophys. Res.*, 110(D22), 2005.

[9] Vivien Mallet and Bruno Sportisse. Uncertainty in a chemistry-transport model due to physical parameterizations and numerical approximations: an ensemble approach applied to ozone modeling. *J. Geophys. Res.*, 111(D01302), 2006.

[10] Denis Quélo, Vivien Mallet, and Bruno Sportisse. Inverse modeling of NO_x emissions at regional scale over Northern France. Preliminary investigation of the second-order sensitivity. *J. Geophys. Res.*, 110(D24310), 2005.

[11] Vivien Mallet and Bruno Sportisse. Toward ensemble-based air-quality forecasts. *J. Geophys. Res.*, 2006. Accepted for publication.

[12] Y. Roustan and M. Bocquet. Sensitivity analysis for mercury over Europe. *J. Geophys. Res.*, 2006. Accepted for publication.

[13] Y. Roustan and M. Bocquet. Inverse modeling for mercury over Europe. *Atmos. Chem. Phys. Discuss.*, pages 795–838, 2006. SRef-ID: 1680-7375/acpd/2006-6-795.

[14] J.P. Issartel. Rebuilding sources of linear tracers after atmospheric concentration measurements. *Atmos. Chem. Phys.*, (3):3111–3125, 2003.

[15] M. Bocquet. Reconstruction of an atmospheric tracer source using the principle of maximum entropy II : Applications. *Quart. J. Roy. Meteor. Soc.*, 131(Part B(610)), 2005.

[16] B. Baklanov and J.H. Sorensen. Parameterisation of radionuclides deposition in atmospheric long-range transport modelling. *Phys.Chem.Earth(B)*, 26(10):787:799, 2001.

[17] S. Galmarini, R. Bianconi, W. Klug, T. Mikkelsen, R. Addis, S. Andronopoulos, P. Astrup, A. Baklanov, J. Bartniki, J. C. Bartzis, et al. Ensemble dispersion forecasting – part I: concept, approach and indicators. *Atmos. Env.*, 38(28):4,607–4,617, 2004.

[18] S. Galmarini, R. Bianconi, R. Addis, S. Andronopoulos, P. Astrup, J. C. Bartzis, R. Bellasio, R. Buckley, H. Champion, M. Chino, et al. Ensemble dispersion forecasting – part II: application and evaluation. *Atmos. Env.*, 38(28):4,619–4,632, 2004.

[19] L. Robertson and C. Perrson. Attempts to apply four dimensional data assimilation of radiological data using the adjoint technique. *Radiation Protection Dosimetry*, 50(2-4):333:337, 1993.

[20] M. Krysta, M. Bocquet, O. Isnard, J.P. Issartel, and B. Sportisse. Data assimilation of radionuclides at short and regional scales. In *Proceedings of the Workshop on Environmental security*. NATO, Kluiwer, 2004.

[21] D. Quélo, B. Sportisse, and O. Isnard. Data assimilation for short-range dispersion of radionuclides: a case study for second-order sensitivity. *J.Environ.Radioactivity*, 84:393–408, 2005.

[22] J.F. Louis. A parametric model of vertical eddy fluxes in the atmosphere. *Boundary-Layer Meteor.*, 17:197:202, 1979.

[23] J.G. Verwer, W.H. Hundsdorfer, and J.G. Blom. Numerical time integration for air pollution models. In *Proceedings of the Conference APMS'98*. ENPC-INRIA, October 26-29 1998.

[24] A. Pourchet, V. Mallet, D. Quélo, and B. Sportisse. A review of some numerical issues in Chemistry-Transport models. Submitted to J.Comp.Phys., September 2006.

[25] R. Pöllänen, I. Valkama, and H. Toivonen. Transport of radioactive particles from the Chernobyl accident. *Atmos. Env.*, 31(21):3575–3590, 1997.

[26] A. Baklanov. Parameterisation of the deposition processes and radioactive decay: a review and some preliminary results with the DERMA model. Technical Report 99-4, DMI, 1999.

[27] JRC. ETEX, the European Tracer EXperiment: comprehensive overview of the ETEX project. Technical report, Joint Research Center, 1998.

[28] K. Nodop, editor. *ETEX symposium on long-range atmospheric transport, model verification and emergency response*, May 1997. Vienna (Austria).

[29] L. Robertson and J Langner. Variational assimilation of ETEX-I data. In K. Nodop, editor, *Proceedings of the ETEX Symposium on long-range atmospheric transport, model verification and emergency response*, 1997.

[30] L. Robertson and J. Langner. Source function estimate by means of adjoint variational data assimilation applied to the ETEX-I tracer experiment. *Atmos. Env.*, 32(24):4219–4225, 1998.

[31] J.P. Issartel and J. Baverel. Adjoint backtracking for the verification of the comprehensive test ban treaty. *Atmos. Chem. Phys. Discuss.*, 2:2133:2150, 2002.

[32] M. Bocquet. Grid resolution dependence in the reconstruction of an atmospheric tracer source. *Nonlinear Process in Geophysics*, 12, 2005.

[33] J. Brandt. *Modelling Transport, Dispersion and Deposition of Passive Tracers from Accidental Releases.* PhD thesis, NERI, Denmark, 1998.

[34] UNSCEAR Report. Annex J: exposure and effects of the Chernobyl accident, 2000.

[35] P.J. Vogt, B.M. Pognaz, F.J.Aluzzi, R.L.Baskett, and T.J.Sullivan. ARAC Simulation of the Algeciras, Spain Steel Mill Cs-137 Release. Technical Report JC-131330, Lawrence Livermore National Laboratory, USA, 1998.

[36] R. L. Buckley. Modeling Atmosperic Deposition from a Cesium Release in Spain Using a Stochastic Transport Model. Technical report, Westinghouse Savannah River Company, USA, 1999.

[37] G. Graziani, S. Galmarini, and T. Mikkelsen. RTMOD: Real-Time MODel Evaluation. Technical report, Risøe, Denmark, 2000.

[38] S. Mosca, G. Graziani, W. Klug, R. Bellasio, and R Bianconi. A statistical methodology for evaluation of ling-range dispersion models : An application to the ETEX exercise. *Atmos. Env.*, 41(24):4307–4324, 1998.